QUASI-CLASSICAL DYNAMICS OF HYDROGEN MOLECULES TRAPPED INSIDE FULLERENE CAGES

DINÁMICA CUASI-CLÁSICA DE MOLÉCULAS DE HIDRÓGENO ATRAPADAS EN FULERENOS

J. A. Heredia-Kindelán[a,c], L. D. Fernández-Quintana[a,c], N. Halberstadt[b], L. Uranga-Piña[b,c], A. Martínez-Mesa[c†]

a) Departamento de Física, Universidad de Oriente, Santiago de Cuba, Cuba.
b) Laboratoire Collisions Agrégats Réactivité (FeRMI), Université de Toulouse III and CNRS, UMR 5589, F-31062 Toulouse Cedex 09, France.
c) DynAMoS (Dynamical processes in Atomic and Molecular Systems), Facultad de Física, Universidad de la Habana, La Habana, Cuba. aliezer@fisica.uh.cu†
† corresponding author

Recibido 19/1/2025; Aceptado 31/5/2025

We perform molecular dynamics simulations of hydrogen molecules inside fullerene cages, incorporating quantum effects via the Feynman-Hibbs effective potential method. The distance between hydrogen atoms in the molecule is kept fixed by using the constraint dynamics algorithm. We evaluate the energetic properties and the influence of quantum effects for hydrogen molecules in fullerene cages of varying size and geometry (C_n, $n = 24, 28, 60, 70$), and within a wide range of thermodynamics conditions (i.e., from $T = 130$ K to $T = 320$ K). We compute the temperature dependence of quantities such as the translational and rotational kinetic energies, the total energy and the contribution of quantum effects. It is found that quantum corrections to the total energy are significant even at room temperature. We discuss the possible influence of these properties on the hydrogen storage capacity of these materials.

Simulamos la dinámica de moléculas de hidrógeno dentro de fulerenos en forma de jaula, incorporando los efectos cuánticos mediante el método del potencial efectivo de Feynman-Hibbs. La distancia entre los átomos de hidrógeno se mantiene fija utilizando el método de dinámica molecular con ligaduras. Evaluamos las propiedades energéticas y la influencia de los efectos cuánticos de moléculas de hidrógeno en fulerenos de distintos tamaños y geometrías (C_n, $n = 24, 28, 60, 70$), dentro de un rango amplio de condiciones termodinámicas ($T = 130$ K hasta $T = 320$ K). Se estudió la dependencia, con respecto a la temperatura, de magnitudes como las energías cinéticas de traslación y de rotación, la energía total y la contribución de los efectos cuánticos. Se determinó que las correcciones cuánticas a la energía son significativas incluso a temperatura ambiente. Discutimos la posible influencia de estas propiedades sobre el almacenamiento de hidrógeno en estos materiales.

Keywords: Molecular dynamics simulations (Simulaciones de dinámica molecular); Semiclassical molecular dynamics (dinámica molecular semiclásica); Hydrogen storage (almacenamiento de hidrógeno).

I. INTRODUCTION

Today, hydrogen is considered one of the main alternatives to fossil fuels for mobile applications [1]. Hydrogen is an environmentally friendly renewable energy carrier with promising applications in various sectors. For example, efforts are underway to adopt hydrogen as a fuel in transportation, stationary and portable back-up power plants, power supply to off-grid areas, among other usages [2].

Despite its high energy density and environmentally safe nature, large-scale exploitation of hydrogen as a fuel constitutes a challenge for modern science, particularly concerning safe and efficient hydrogen storage for mobile applications. Various technologies have been developed to store hydrogen, such as compressed hydrogen gas tanks, liquefaction, chemically in the form of solid hydrides or by spillover of hydrogen, or by physical adsorption in porous materials [2–6]. Currently, none of these methods can meet the current reference U.S. Department of Energy goals for efficient on-board hydrogen storage, or they bear high energy consumption or high material costs [1].

Physisorption on nanostructured surfaces is one of the most promising alternatives to store hydrogen due to the typically high energy density attained, the reversibility, and the fast kinetics [7]. Specifically, hydrogen uptake by carbon-based nanomaterials provides valuable insight into the microscopic mechanisms underlying the adsorption process. The wide variety of thermodynamically stable carbon allotropes enables several parameters, such as the pore size and the binding energy, to be tuned almost continuously. Therefore, despite exhibiting lower storage capacities than more complex materials (for example, metal-organic and covalent-organic frameworks), carbonaceous materials remain as widespread model systems for studying H_2 physisorption [8].

While several authors addressed the evaluation of quantum effects on hydrogen physisorption within the featureless particle approximation (see [9], and references therein), studies of rotational quantum dynamics of adsorbed hydrogen molecules are scarce in the literature [10].

The purpose of this paper is to investigate the quasi-classical dynamics of hydrogen molecules encapsulated in fullerene cages of varying sizes, with a focus on the energetics and the emergence of quantum effects. Fullerenes constitute paradigmatic examples of curved carbon nanostructures. They can be regarded as the elementary building blocks of fullerites, which are appealing as hydrogen storage

media [11]. In Section *Methodology*, we describe the computational approach to effective potential molecular dynamics simulations of H_2 molecules inside fullerene cages. The computed energetic properties of endohedral $H_2@C_n$ molecules are presented in section *Results and discussion*. The main findings and some perspectives are summarized in section *Conclusions*.

II. METHODOLOGY

Within the constraint dynamics method [12], the positions of the hydrogen atoms obey the following equations of motion:

$$m\ddot{\vec{r}}_i = \vec{f}_i + \vec{\gamma}_{ij}(t), \tag{1}$$

where $\vec{r}_i$ $(i = 1, 2)$ is the position of the hydrogen atom *ith*, $\vec{f}_i$ is the force exerted on each H atom by the fullerene cage and m is the hydrogen atomic mass. The symbols $\vec{\gamma}_{ij}$ $(i \neq j)$ denote intramolecular constraint forces introduced to keep the distance between hydrogen atoms constant, that is, at each point in time:

$$|\vec{r}_{12}(t + \Delta t)|^2 = |\vec{r}_{21}(t + \Delta t)|^2 = l^2. \tag{2}$$

Here, $\Delta t = 1$ fs is the time step, $l = 0.74$ Å is the equilibrium bond distance in the hydrogen molecule.

The positions $\vec{r}_i$ and velocities $\vec{v}_i$ are propagated as follows:

$$\vec{r}_i(t + \Delta t) = \vec{r}_i(t) + \vec{v}_i(t)\Delta t + \frac{1}{2}\vec{a}_i(t)\Delta t^2, \tag{3}$$

$$\vec{v}_i(t + \Delta t) = \alpha\vec{v}_i(t) + \frac{1}{2}\left[\vec{a}_i(t) + \vec{a}_i(t + \Delta t)\right]\Delta t, \tag{4}$$

where $\vec{a}_i(t) = -\nabla_i V(\vec{r})/m$ is the instantaneous acceleration of the *ith* particle. The vector $\vec{r} = (\vec{r}_1, \vec{r}_2)$ represents the positions of the two hydrogen atoms.

Equations (3) and (4) correspond to the velocity Verlet algorithm [12], augmented by introducing the velocity rescaling factor:

$$\alpha = \sqrt{\frac{K_t}{K}}, \tag{5}$$

which enforces the canonical distribution of the total kinetic energy of the system. The target value K_t of the kinetic energy is drawn randomly from the canonical equilibrium distribution for the kinetic energy [13]:

$$\bar{P}(K_t)dK_t \propto K_T^{N_f/2-1} e^{-\beta K_t} dK_t. \tag{6}$$

N_f is the total number of degrees of freedom in the system.

The interaction potential V between the hydrogen molecule and the (frozen) host structure is modeled as a superposition of pairwise interactions of the form:

$$V(\vec{r}) = \sum_{i,\nu}\left[Ae^{-a|\vec{r}_i - \vec{r}_\nu|} - \frac{C}{\left|\vec{r}_i - \vec{r}_\nu\right|^6}\right], \tag{7}$$

where A, a, and C are constant parameters fitted to ab initio data: $A = 12676$ kcal·mol^{-1}, $a = 3.5763$Å^{-1}, $C = 200.185$ kcal·mol^{-1}Å^6 [14]. $\vec{r}_\nu$ is the position of each carbon atom in the fullerene cage.

The well depth of the C-H pair potential in equation (7) is $6.3 \cdot 10^{-2}$ kcal·mol^{-1}, and the minimum is attained at an interatomic separation of 3.4 Å. Comparatively, the equilibrium C-H distance is 1.46, 1.28, 0.97, and 0.89 times larger than the cage radii of C_{24}, C_{28}, C_{60}, and C_{70} fullerenes, respectively [15]. Therefore, we can expect guest molecules to be tightly confined by repulsive forces at the centre of the C_{24} and C_{28} cages, while the two larger fullerenes display interaction potential minima at the centre of the cavity (for C_{60}), and slightly displaced from the centre (for C_{70}).

As a result of the mismatch between the frequency of the host phonons and the characteristic time scale of the guest molecule motion, the influence of the vibrations of carbon atoms on the computed thermodynamic properties is negligible (within the investigated temperature range). A similar result has been verified for hydrogen storage in carbonaceous nanomaterials, e.g., using frozen phonon models [25]. Therefore, the results reported in following section were obtained assuming a frozen host structure.

In order to account for quantum effects at finite temperature within a molecular dynamics framework, we consider atoms moving on the Feynman-Hibbs effective potential:

$$V_{FH}(\vec{r}) = V(\vec{r}) + \frac{\beta\hbar^2}{24m}\sum_i \nabla_i^2 V(\vec{r}). \tag{8}$$

In equation (8), ∇_i^2 is the Laplacian operator with respect to the coordinates of particle i, $\beta = \frac{1}{k_B T}$ is the inverse temperature, k_B is the Boltzmann constant, and $\hbar$ is the Planck's constant.

The Feynman-Hibbs effective potential has been extensively used to incorporate moderate quantum effects [23, 24]. The second, temperature-dependent term in equation (8) accounts for the effects of quantum delocalization, i.e., it corresponds to the path integral average of position-dependent observables around the classical path, over a region of size equal to the De Broglie thermal wavelength $\sqrt{2\pi\beta\hbar^2/m}$.

For each fullerene cage and for every temperature T, the simulation procedure can be summarized as follows. A hydrogen molecule with random orientation is initially placed inside the carbon framework. The initial position of the molecular centre of mass is assigned randomly around the center of the cage, following a three-dimensional Gaussian distribution of standard deviation equivalent to 40 % of the cage radius. Initial velocities of the centre of mass along each Cartesian axis are drawn from the corresponding Maxwell-Boltzmann distribution. Upon thermalization, properties are calculated as averages over trajectories starting from 40 different initial conditions. In turn, each trajectory is propagated for 150,000 simulation steps.

Furthermore, we examine the validity of a simple model of $H_2@C_{60}$ and $H_2@C_{70}$ endohedral molecules, consisting of decoupled rotational and centre of mass translational motions. To this purpose, the computed average total energies of H_2 in

C_{60} and C_{70} fullerene cages were fitted to the superposition of the internal energies of a three-dimensional isotropic harmonic oscillator (of mass equal to $2m$, its frequency ω is considered as a fitting parameter):

$$\frac{3}{2}\hbar\omega + \frac{3}{2}\frac{\hbar\omega\, e^{-\beta\hbar\omega}}{1-e^{-\beta\hbar\omega}}, \tag{9}$$

and of a free rigid rotor (with rotational constant B_e) [22]:

$$-\frac{\partial}{\partial\beta}\left[\frac{3}{4}\ln\left\{\sum_{l\ even}(2l+1)e^{-\beta B_e l(l+1)}\right\} + \frac{1}{4}\ln\left\{\sum_{l\ odd}(2l+1)e^{-\beta B_e l(l+1)}\right\}\right]. \tag{10}$$

In practice, the sums in equation (10) were approximated with the first three non-zero terms.

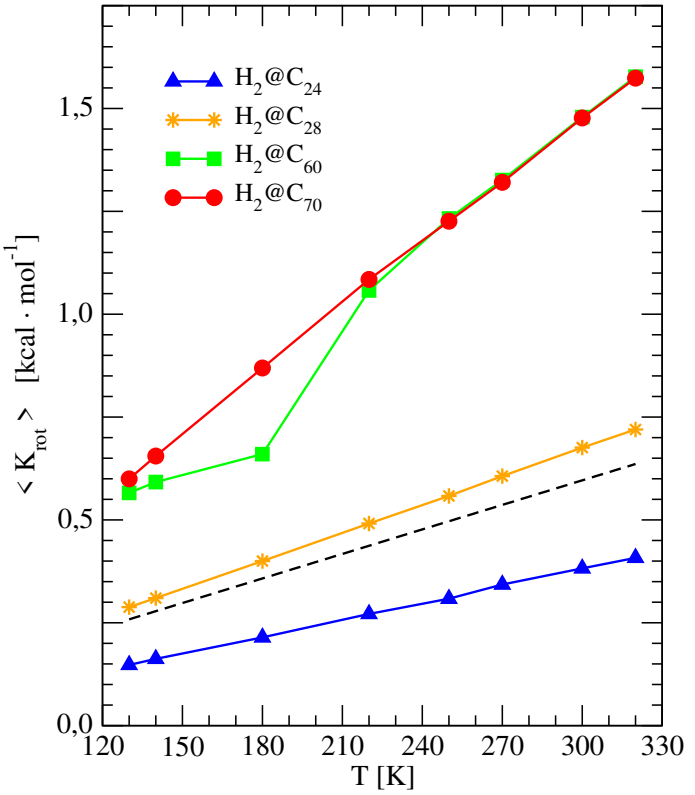

Figure 1. Average rotational kinetic energy $\langle K_{rot}\rangle$ of hydrogen molecules encapsulated in C_{24} (up triangles), C_{28} (stars), C_{60} (squares), and C_{70} (circles), as a function of temperature. The dashed line represents the temperature dependence of the rotational energy of H_2, as predicted by the energy equipartition theorem.

III. RESULTS AND DISCUSSION

In the following, we present the characterization of the energetics of $H_2@C_n$ endohedral fullerenes (n = 24, 28, 60, 70) in the range of temperatures from 130 K up to 320 K.

For each system, the computed total kinetic energy (translational plus rotational) is equal to $N_f/2\beta$, up to numerical fluctuations. However, due to the emergence of quantum effects, the kinetic energy is not evenly partitioned among all degrees of freedom at thermal equilibrium.

Figure 1 illustrates the influence of the confinement potential on the rotational motion of the guest molecule. It can be noticed that H_2 rotation is subject to larger energy barriers in the smaller fullerenes. Still, due to the small bond length of H_2, the molecule is able to complete rotations even in the smallest C_{24} cage.

On the one hand, the rotational energy of H_2 molecules trapped inside C_{24} and C_{28} cages remains rather close and increases with a slope similar to that predicted by the energy equipartition principle, at all temperatures. On the other hand, the rotational energy of hydrogen molecules in C_{60} and C_{70} fullerenes is higher than anticipated by the equipartition theorem. For these two fullerenes, the $\langle K_{rot}\rangle(T)$ curves present steeper slopes on average, compared both to the energy equipartition theorem and the smaller C_{24} and C_{28} cages. It can be seen that the average rotational energy of H_2 is very similar in C_{60} and C_{70} above 220 K, while the former is somewhat lower for temperatures between 130 K and 180 K.

This behaviour can be rationalised by considering the differences in the confinement potential exerted on H_2 molecules by the host structures. The equilibrium position of the H_2 molecule was at the centre of the cavity in C_{60}, whereas two symmetrical equilibrium positions were observed near the centre of the cage in C_{70}, oriented along the major axis. As a consequence of the nearly spherical symmetry, and the size of the buckminsterfullerene (the cage radius is 3.53Å) and C_{70} (geometrical mean radius of 3.83Å), the encapsulated hydrogen molecule behaves almost as a free rotor. Featuring the largest molecular rotational constant in nature (B_e/k_B = 87.17 K), the energy spacing between low-lying rotational levels of the free H_2 molecule (i.e., $2B_e$, $4B_e$, $6B_e$, ...) are similar to or larger than k_BT within the range of thermodynamic conditions investigated here.

The discrete character of the rotational spectra of the encapsulated molecule lies at the origin of the observed deviations from the energy equipartition principle. Although the Feynman-Hibbs method can not take the discrete character of the molecular rotational spectra into account explicitly, the method has been shown to accurately reproduce thermodynamic properties (e.g., the free energy) even in the ultra-quantum limit (i.e., for $E_{n+1} - E_n \gg k_BT$, where n represents a collective quantum number labelling the energy levels of the system) [17].

For the C_{24} and C_{28} cavities, rotational hindering by the anisotropic hydrogen-cage interaction potential creates a higher density of rotational states within the thermal and

subtermal energy regions, and the behaviour predicted by the energy equipartition theorem is approximately recovered. It can be seen, that within the investigated temperature range, the tighter the confinement imposed by the host structure, the smaller the rotational energy of hydrogen molecules encapsulated in the cavity.

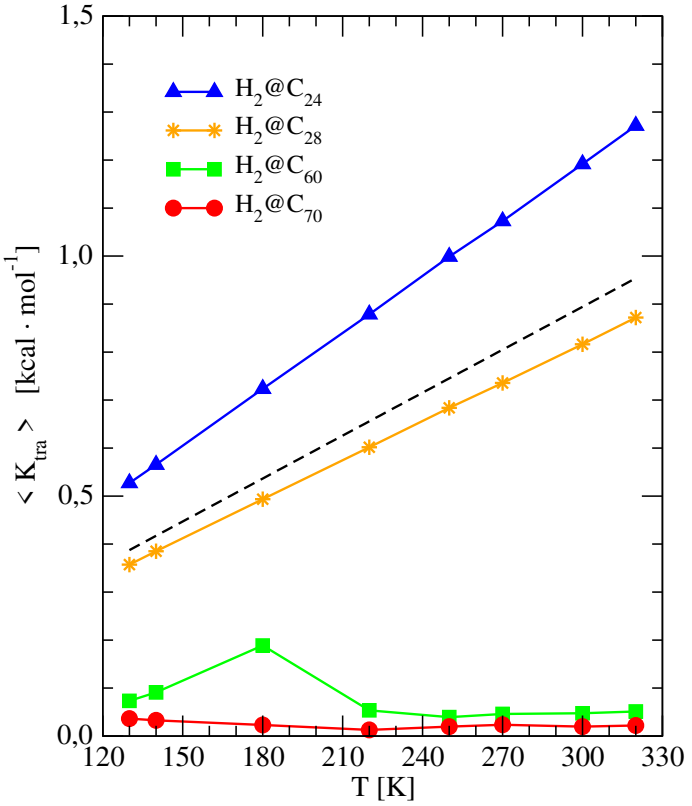

Figure 2. Average translational kinetic energy $\langle K_{tra} \rangle$ of H_2 molecules encapsulated in fullerene cages (C_{24}, C_{28}, C_{60}, and C_{70}), as a function of temperature. The dashed line represents the temperature dependence of the translational energy of H_2, as predicted by the energy equipartition theorem.

In figure 2, we show the average translational kinetic energy $\langle K_{tra} \rangle$ of hydrogen molecules trapped in the fullerene cages. Since the total kinetic energy is proportional to temperature, the temperature dependence of $\langle K_{tra} \rangle$ mirrors that of the average rotational energy. That is, for hydrogen molecules in C_{24} and C_{28}, $\langle K_{tra} \rangle(T)$ increases linearly following a similar trend to that predicted by the energy equipartition theorem. Conversely, the temperature-dependent, average translational kinetic energy of H_2 in C_{60} and C_{70} is comparatively smaller and flatter than for the two smallest fullerenes.

This trend suggests that nanoporous materials displaying inner cavities with sizes and shapes resembling C_{60} and C_{70} cages would be more suitable as hydrogen storage media. Indeed, in these nanostructures, a larger fraction of thermal energy takes the form of rotational rather than translational energy of H_2 molecules. This property translates in smaller vibrational amplitudes of guest molecules around their equilibrium positions in the cage. Since the equilibrium distance of the isotropic average of H_2-H_2 intermolecular interaction is 3.4Å [18], both C_{60}- and C_{70}-like pores can accommodate two H_2 molecules, at the expense of somewhat increased barriers to rotation due to the interaction with pore walls.

The influence of quantum effects on the energetics of $H_2@C_n$ endohedral molecules can be quantified in terms of the extent of the temperature-dependent contribution in the Feynman-Hibbs potential (equation (8)). The plots in figure 3 show that quantum effects are at least one order of magnitude larger in C_{24} and C_{28}, compared to C_{60} and C_{70}, owing to the tightest confinement imposed by the smaller nanostructures on the guest molecules.

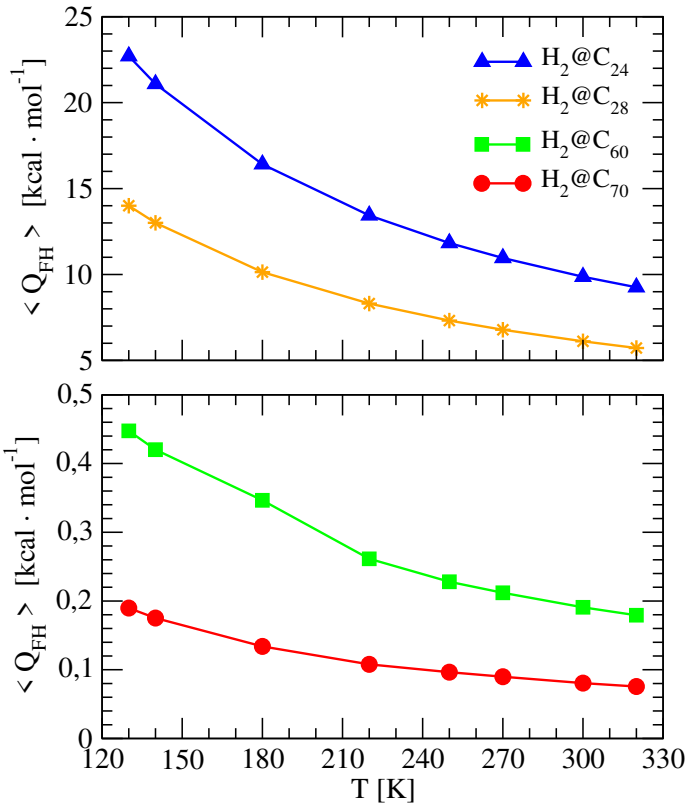

Figure 3. Average quantum contribution $\langle Q_{FH} \rangle$ in the effective Feynman-Hibbs potential for $H_2@C_n$ (n = 24, 28, 60, 70), as a function of temperature.

The magnitude of quantum effects gradually decreases as temperature gets larger, i.e, at T = 320 K, the average quantum contribution to the effective potential drops down to 41 % of its value at T = 130 K, for hydrogen trapped inside C_{24} and C_{28} cages. Within the same interval of temperature, the size of this contribution declines by 43 % and 50 % for the C_{60} and C_{70} fullerenes respectively.

In figure 4, we show the total energy of encapsulated H_2 molecules as a function of temperature. It can be seen that this quantity behaves quite differently in response to cage size.

In C_{24} and C_{28}, guest molecules are confined by repulsive interactions with the cage walls. The hydrogen molecules trapped in these structure undergo a 7% reduction of their total energy when temperature increases from T = 130 K up to 320 K. Such diminution owes chiefly to the reduction of the temperature-dependent contribution to the effective Feynmann-Hibbs potential by 60 % (13.4 kcal·mol^{-1} and 8.3 kcal·mol^{-1} for $H_2@C_{24}$ and $H_2@C_{28}$, respectively).

The Feynmann-Hibbs quantum correction gets smaller as a consequence of the decrease of the De Broglie thermal wavelength.

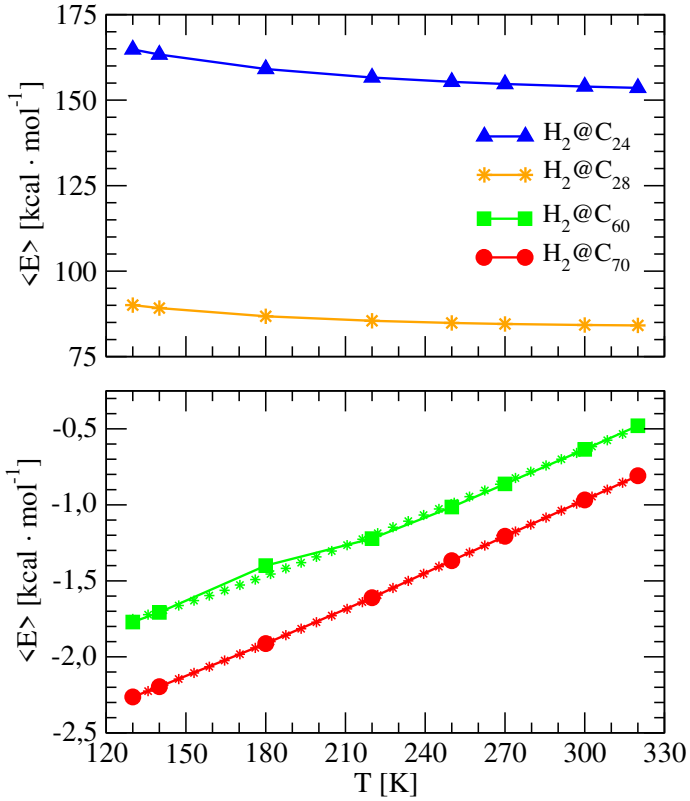

Figure 4. Average total energy ⟨E⟩ of H_2 molecules trapped in C_{24}, C_{28}, C_{60}, and C_{70} fullerene cages, as a function of temperature. In the bottom panel, star symbols correspond to the fitting to the sum of internal energies of a three-dimensional isotropic harmonic oscillator and a free rigid rotor ((equations (9) and (10)).

Notably, quantum effects are non negligible for H_2 molecules in fullerene cages, even at room temperature. Indeed, quantum corrections amount to 14 % and 16 % of the total energy at T = 130 K in C_{24} and C_{28} cages, respectively, and their participation reduces down to 6 % and 7 % at T = 320 K.

Inside C_{60} and C_{70} fullerenes, hydrogen molecules remain bound to the cage below room temperature. At T = 130 K, the average adsorption energy is 1.8 kcal·mol^{-1} in the buckminsterfullerene, and 2.3 kcal·mol^{-1} in C_{70}. The binding energy monotonously decreases as temperature rises, which indicates a gradual deterioration of the hydrogen storage capacities of cage-like fused-ring carbon nanostructures within this temperature range.

As expected, the quantum correction to the total energy decrease with temperature. In C_{60}, this contribution reduces from 0.45 kcal·mol^{-1} at T = 130 K to 0.18 kcal·mol^{-1} at T = 320 K. In C_{70} fullerenes, it decreases from 0.19 kcal·mol^{-1} at T = 130 K down to 0.08 kcal·mol^{-1} at T = 320 K.

The computed total energies ⟨E⟩(T) of the H_2@C_{60} and H_2@C_{70} endohedral molecules are well reproduced by the sum of the internal energies of a three-dimensional isotropic harmonic oscillator and a rigid rotor (equations (9) and (10), respectively, see bottom panel in figure 4). The fitting scheme yields values ω = 404.2 K and 221.8 K for the energy spacing between translational energy levels in C_{60} and C_{70}, respectively. The deviation between the results of the fitting and previous experimental and theoretical evaluations of the fundamental vibrational frequency of H_2 centre of mass in these fullerenes are within 1 % and 15 % [10, 19–21]. This level of agreement is satisfactory, considering that the functional form employed in the fitting does not account for the anharmonicity and weak anisotropy of the confining potential, nor the coupling between orbital and rotational angular momenta, and that the results of previous experimental and theoretical calculations show notable variations [20].

IV. CONCLUSIONS

We report quasi-classical simulations of the translational and rotational dynamics of hydrogen molecules inside four quasi-spherical fullerene cages, namely C_{24}, C_{28}, C_{60}, and C_{70}. Energetic properties are computed from 130 K to 320 K, covering a sizable part of the temperature range of interest for storage technology applications.

The rise in temperature causes the average rotational and translational kinetic energies of embedded hydrogen molecules to increase (roughly) linearly. The energy spacing between adjacent low-lying rotational levels of the H_2 molecule in buckminsterfullerene and in C_{70} is comparable to or greater than k_BT, which causes deviations from the energy equipartition principle. Overall, the influence of quantum delocalization on energetic properties remains non-negligible over the entire range of thermodynamic conditions investigated here.

Novel materials featuring highly ordered and randomly packed assemblies of carbon nanocages have recently been synthesized and investigated with respect to their potential applications for energy storage and conversion [16]. The connection between the energetics of endohedral H_2@C_n molecules, and the hydrogen storage capacities of these carbon-based nanostructures is as follows.

In these materials, efficient hydrogen uptake can only be achieved if there are enough large pores. For these fullerenes, the H_2-surface interaction prevents adsorption. As it happens, the tight confinement imposed on the H_2 molecules by the smaller host structures (C_{24}, C_{28}) triggers marked quantum delocalization effects.

Nanocavities resembling C_{60} and C_{70} appear to be suitable hydrogen storage media, since hydrogen molecules remain bound to the cage for temperatures up to room temperature. The hydrogen storage capacities of C_{60}- and C_{70}-like nanocages will result from a trade-off between the higher binding energy of hydrogen to the host structure, and the possibility to accommodate more than one guest molecule per pore, owing to the smaller vibrational amplitude of H_2 translational motion in the cage.

Based on the present results, we plan in the future to extend the methodology to model hydrogen uptake by more complex nanomaterials (e.g., assemblies of carbon nanocages, metal- and covalent-organic frameworks) in the high-density regime

(i.e., by including several interacting H_2 molecules). In this perspective, the motion of host atoms may become relevant for more flexible nanoporous materials. Within the present approach, the inclusion of vibrations of host structure is straightforward. Work along this line is underway.

V. ACKNOWLEDGEMENTS

The results incorporated in this publication have received funding from the European Union's Horizon 2020 and Horizon Europe research and innovation programmes, under the Marie Skłodowska-Curie grant agreements n^{o}898663, and n^{o}101155733, respectively.

REFERENCES

[1] Q. Hassan, A. Z. Sameen, H. M. Salman, M. Jaszczur, and A. K. Al-Jiboory, *J. Energy Storage* **72**, 108404 (2023).

[2] H. Barthélemy, M. Weber, and F. Barbier, *Int. J. Hydrogen Energy* **42**, 7254 (2017).

[3] S. Satyapal, J. Petrovic, C. Read, G. Thomas, and G. Ordaz, *Catal. Today* **120**, 246 (2007).

[4] N. A. A. Rusman and M. Dahari, *Int. J. Hydrogen Energy* **41**, 12108 (2016).

[5] H. Shen, H. Li, Z. Yang, and C. Li, *Green Energy Environ.* **7**, 1161 (2022).

[6] M. Hirscher, A. Züttel, A. Borgschulte, and L. J. C. T. Schlapbach, (2009) Handbook of hydrogen storage. *Ceramic Transactions*, 202.

[7] M. Bastos-Neto, C. Patzschke, M. Lange, J. Möllmer, A. Möller, S. Fichtner, C. Schrage, D. Lässig, J. Lincke, R. Staudt, et al., *Energy Environ. Sci.* **5**, 8294 (2012).

[8] M. Mohan, V. K. Sharma, E. A. Kumar, and V. Gayathri, *Energy Storage* **1**, e35 (2019).

[9] A. Martínez-Mesa and G. Seifert, *Rev. Cubana Fis.* **31**, 32 (2014).

[10] Z. Bačić, *J. Chem. Phys.* **149**, 100901 (2018).

[11] N. S. Venkataramanan, H. Mizuseki, and Y. Kawazoe, *Nano* **4**, 253 (2009).

[12] J.-P. Hansen and I. R. McDonald, *Theory of Simple Liquids: With Applications to Soft Matter* (Academic Press, 2013).

[13] G. Bussi, D. Donadio, and M. Parrinello, *J. Chem. Phys.* **126**, 014101 (2007).

[14] T. Heine, L. Zhechkov, and G. Seifert, *Phys. Chem. Chem. Phys.* **6** (2004).

[15] G. B. Adams, M. O'Keefe, and R. S. Ruoff, *J. Phys. Chem.* **98** (1994).

[16] B. Rodríguez-Hernández, T. Nelson, N. Oldani, A. Martínez-Mesa, L. Uranga-Piña, Y. Segawa, S. Tretiak, K. Itami, and S. Fernandez-Alberti, *J. Phys. Chem. Lett.* **12**, 224 (2021).

[17] R. P. Feynman and A. R. Hibbs, *Quantum Mechanics and Path Integrals* (McGraw-Hill College, 1965).

[18] U. K. Deiters and R. J. Sadus, *J. Chem. Phys.* **158** (2023).

[19] M. Ge, U. Nagel, D. Hüvonen, T. Rõõm, S. Mamone, M. H. Levitt, M. Carravetta, Y. Murata, K. Komatsu, J. Y.-C. Chen, and N. J. Turro, *J. Chem. Phys.* **134** (2011).

[20] M. Xu, F. Sebastianelli, Z. Bačić, R. Lawler, and N. J. Turro, *J. Chem. Phys.* **129** (2008).

[21] F. Sebastianelli, M. Xu, Z. Bačić, R. Lawler, and N. J. Turro, *J. Am. Chem. Soc.* **132** (2010).

[22] M. Capitelli, G. Colonna, and A. D'Angola, *Fundamental Aspects of Plasma Chemical Physics: Thermodynamics* (Springer Science, 2012).

[23] R. Rodríguez-Cantano, R. Pérez de Tudela, M. Bartolomei, M. I. Hernández, J. Campos-Martínez, T. González-Lezana, P. Villarreal, J. Hernández-Rojas, and J. Bretón, *J. Phys. Chem. A* **120**, 034302 (2016).

[24] O. Elafifi, N. Tchouar, K. Ouadah, and M. Arab Ait Tayeb, *Int. J. Mod. Phys. B* **38**, 2450296 (2024).

[25] S. Patchkovskii and T. Heine, *Phys. Chem. Chem. Phys.* **9**, 2697 (2007).